Transport and uptake effects of marine complex lipid liposomes in small intestinal epithelial cell models

Lei Du[a†], Yu-Hong Yang[a†], Jie Xu[b], Yu-Ming Wang[b*], Chang-Hu Xue[b], Hideyuki Kurihara[a], Koretaro Takahashi[a*].

[a]Faculty of Fisheries Sciences, Hokkaido University (3-1-1 Minato-cho, Hakodate, Hokkaido 041-8611, Japan)

[b]College of Food Science and Engineering, Ocean University of China (No.5 Yu-Shan Road, Qingdao, Shandong Province, 266003, People's Republic of China)

[†]These authors contributed equally to this work.

[*]To whom correspondence should be addressed:

Koretaro Takahashi

Tel: +81-138-40-5560, Fax: +81-0138-40-5560. E-mail address: kore@fish.hokudai.ac.jp

Yu-Ming Wang

Tel: +86-532-82032597, Fax: +86-532-82032468. E-mail address: wangyuming@ouc.edu.cn

Abbreviations

AP, apical; BL, basolateral; Chol, cholesterol; EPA, eicosapentaenoic acid; EPA-PL, EPA-enriched phospholipids; DHA, docosahexaenoic acid; FAE, follicle-associated epithelium; GC-MS, gas chromatography-mass spectrometry; HBSS, Hanks balanced salt solution; LY, Lucifer yellow; PBS, phosphate buffered saline; PC, phosphatidylcholine; PLs, phospholipids; PUFAs, polyunsaturated fatty acids; SCC, sea cucumber cerebrosides; SCP, sea cucumber phospholipids; SEM, scanning electron microscopy; SFC, starfish cerebrosides; SFP, starfish phospholipids; soy-PL, soy phospholipids; TEER, transepithelial electrical resistance.

Abstract

Nowadays, the marine complex lipids, including starfish phospholipids (SFP) and cerebrosides (SFC) separated from *Asterias amurensis* as well as sea cucumber phospholipids (SCP) and cerebrosides (SCC) isolated from *Cucumaria frondosa* have received much attention because of their potent biological activities. However, little information has been known on the transport and uptake of these lipids in liposome forms in small intestinal cells. Therefore, this study was undertaken to investigate the effects of these complex lipids liposomes on transport and uptake in Caco-2 and M cell monolayer models. The results revealed that SFP and SCP contained 42 % and 47.9 % eicosapentaenoic acid (EPA), respectively. The average particle sizes of liposomes prepared in this study were from 169 to 189 nm. We found that the transport of the liposomes across M cell monolayer model were much higher than Caco-2 cell monolayer model. The liposomes consisted of SFP or SCP showed significantly higher transport and uptake than soy phospholipids (soy-PL) liposomes in both Caco-2 and M cell monolayer models. Our results also exhibited that treatment with 1 mM liposomes composed of SFP or SCP for 3 h tended to increase the EPA content in phospholipid fractions of both differentiated Caco-2 and M cells. Moreover, it was also found that the hybrid liposomes consisted of SFP/SFC/cholesterol (Chol) revealed higher transport and uptake across M cell monolayer in comparison with other liposomes. Furthermore, treatment with SFP/SFC/Chol liposomes could notably decrease the transepithelial electrical

resistance (TEER) values of Caco-2 and M cell monolayers. The present data also showed that the cell viability of differentiated Caco-2 and M cells were not affected after the treatment with marine complex lipid or soy-PL liposomes. Based on the data in this study, it was suggested that marine complex lipid liposomes exhibit prominent transport and uptake in small intestinal epithelial cell models.

Keywords: EPA-enriched phospholipids, cerebrosides, transport, uptake, transepithelial electrical resistance, Caco-2 cells, M cells.

1 Introduction

Recently, the health-beneficial effects of complex lipids derived from marine sources such as n-3 polyunsaturated fatty acids (PUFAs)-enriched phospholipids (PLs) and glycosphingolipids, i.e. cerebrosides have witnessed an upsurge. Besides the beneficial nutritional effects of the n-3 PUFAs and PLs themselves, it has been suggested that PLs are widely used as functional ingredients in pharmaceutical industries [1]. Due to the size and amphiphilic properties, PLs are able to form liposomes which are considered as potential drug carrier systems for drug delivery. Our previous studies have observed that the internal organs and gonads of starfish *Asterias amurensis* and the body wall of sea cucumber *Cucumaria frondosa* are good sources of EPA-enriched phospholipids (EPA-PL) and the contents of EPA in those two PLs are both more than 40 % [2,3]. Although it has been considered that the n-3 PUFAs could alter the intestinal morphology [4], little information has been known on their transport and uptake effects in small intestinal epithelial cells. On the other hand, cerebrosides, another complex and essential class of lipids, which consist of sugars (such as glucose and galactose), an amide-linked fatty acid and a sphingoid base, are also found in marine echinoderms [5]. Cerebrosides have been shown to exhibit variety of biological activities such as antitumor, immunomodulatory, and anti-microbial activities [6–9]. The cerebrosides derived from marine echinoderms such as starfish and sea cucumber have unique sphingoid bases with a conjugated diene such as 2-amino-1,3-dihydroxy-4-heptadecene (d17:1),

2-amino-1,3-dihydroxy-4,8,10-octadecatriene (d18:3) or 2-amino-1,3-dihydroxy-9-methyl-4,8,10-octadecatriene (d19:3) [10,11]. However, to the best of our knowledge, the studies pertaining to the intestinal absorption of cerebrosides derived from marine echinoderms are still lacking.

Human epithelial colorectal adenocarcinoma Caco-2 cells are most commonly used as a model of human intestinal absorption of drugs and other compounds. When cultured as a monolayer, Caco-2 cells differentiate to form tight junctions, microvilli and a number of enzymes and transporters [12]. A study reported the suitability of Caco-2 cell monolayer as a tool to simulate drugs and other compounds transport close to the *in vivo* status [13]. However, it only simulates the epithelial cells in the intestinal epithelium. There are many other cell types including M cells and mucosal cells in the intestine. The lymphoid structures such as the Peyer's patches are separated from the lumen by the follicle-associated epithelium (FAE), which differs from the normal intestinal epithelium in that it contains specialized epithelial M cells with the capacity to transport a broad range of materials [14–16]. It has been suggested that M cells are well established by coculture of Caco-2 cells and B-cell lymphoma Raji cells [17]. And it is desirable that the Caco-2 cell monolayer lose its microvilli thus demonstrating the differentiated Caco-2 cells conversion into M cells.

In the present study, starfish phospholipids (SFP) and cerebrosides (SFC) were separated from *A. amurensis.* Sea cucumber phospholipids (SCP) and cerebrosides (SCC) were isolated from *C. frondosa*. And then the liposomes consisted of these

marine complex lipids were prepared. Next, the Caco-2 cell monolayer model derived from differentiated Caco-2 cells and M cell monolayer model derived from Caco-2 cell monolayer by co-culturing Raji cells were established and validated. Finally, the transport and uptake of marine complex lipid liposomes in those two small intestinal epithelial cell models were investigated.

2 Materials and Methods

2.1 Materials

The starfish *A. amurensis* were collected at the coast of Nemuro, Hokkaido, Japan. The sea cucumber *C. frondosa* were purchased from aquatic products market, Qingdao, China. Soy phospholipids (soy-PL) was supplied from NOF Corporation (Tokyo, Japan). Dulbecco's modified Eagle medium (DMEM), Roswell Park Memorial Institute (RPMI) 1640 medium, fetal bovine serum (FBS), trypsin-EDTA, non-essential amino acids (NEAA) and penicillin streptomycin were obtained from GIBCO (Grand Island, NY, USA). Sodium 2-(4-iodophenyl)-3-(4-nitrophenyl)-5-(2, 4-disulfophenyl)-2H-tetrazolium (WST-1), 1-methoxy-5-methyphenazinium methylsulfate (1-methoxy PMS) and 2-[4-(Hydroxyethyl)-1-piperazinyl] ethanesulfonic acid (HEPES) were supplied from Dojindo Laboratories (Kumamoto, Japan). Calcein, cholesterol, Triton X-100, and L-glutamine were purchased from Wako Pure Chemical Industries, Ltd (Osaka, Japan). Lucifer yellow CH dilithium salt (LY) and fluorescent latex beads (FluoSpheres carboxylate-modified microspheres,

0.2 μm, blue fluorescent 365/415 nm, 2 % solid) were obtained from Molecular Probes (Eugene, Oregon, USA).

2.2 Preparation of phospholipids from starfish and sea cucumber

Phospholipids were extracted from the gonad and viscera of starfish *A. amurensis* as well as the body wall of sea cucumber *C. frondosa* following the modified method of Liu *et al.* [18]. Just in brief, total lipids were extracted following the method of Folch *et al.* [19] and then the extracted lipids were applied to a silica gel column chromatography and eluted with chloroform, acetone and methanol sequentially. Finally, the methanol eluate was collected and evaporated to obtain the PLs. The purity of SFP and SCP were confirmed to be 94.5 % and 93.7 % conducted by normal phase high performance liquid chromatography coupled with an evaporative light scattering detector (HPLC-ELSD) analysis.

2.3 Preparation of cerebrosides from starfish and sea cucumber

The cerebrosides of starfish and sea cucumber were isolated and purified following the method of Xu *et al.* [20] in this study. The cerebrosides was isolated from the less polar lipid fraction of the chloroform-methanol extract using high speed counter-current chromatography (HSCCC) with a two-phase solvent system composed of petroleum ether-methanol-water (5:4:1, v/v/v). The results of purity analysis by HPLC-ELSD showed that the purity of SFC and SCC were 95.2 % and

96.8 %, respectively. The component analysis of cerebrosides and sphingoid base was determined by gas chromatography-mass spectrometry (GC-MS).

2.4 Fatty acid composition analysis of marine and soy phospholipids

The marine and soy PLs were converted to methyl ester derivatives following the method of Prevot and Mordret [21] with slight modifications. The dried sample was dissolved in *n*-hexane and 0.2 mL 2 N-methanolic-NaOH was added. Then, the mixture was shaken, kept at 50 °C for 30 seconds and 0.2 mL 2 N HCl in methanol was added and shaken to neutralize. The mixture was separated by centrifugation at 3000 rpm for 5 minutes. The upper *n*-hexane layer was collected, concentrated, and subjected to gas chromatographic analysis with 0.5 μm thickness PEG-20M liquid phase-coated 40 m × 1.2 mm diameter G-300 column (Chemicals Evaluation and Research Institute, Saitama, Japan) connected to Hitachi 263 gas chromatograph (Hitachi Co. Ltd., Ibaraki, Japan) that was equipped with flame ionization detector. The temperatures of the column, detector, and injection port were 190, 240 and 250 °C, respectively.

2.5 Preparation of liposomes

Liposomes (1 mM) consisted of marine complex lipids or soy-PL were prepared following the method of Bangham [22]. The mixing molar ratios of the composite lipid

classes were SFP/cholesterol (Chol) = 1:1, SCP/Chol = 1:1, SFP/SFC/Chol = 1:1:2, SCP/SCC/Chol = 1:1:2 and soy-PL/Chol = 1:1. The mixtures were dissolved in chloroform and dried to thin film under reduced pressure in a rotary evaporator. The lipid films were hydrated with Hanks balanced salt solution (HBSS) to exfoliate lipid bilayers by vigorous vortex mixing for 5 min. The obtained liposomes suspension was extruded 21 times through polycarbonate membrane filter (Whatman Inc. Newton, MA, USA) with pore size of 200 nm. The size distribution of liposomes was determined using a dynamic light scattering particle size analyzer LB-500 (HORIBA, Kyoto, Japan).

2.6 Characterization of liposomes

The liposomes suspension (40 µL) were added in 10 mM Tris-HCl buffer (2.0 mL, 145 mM NaCl, pH 7.4) containing 0.1 mM calcein to form the calcein-liposomes suspension. The fluorescent intensity of calcein (F_t) was determined by Hitachi F-2500 fluorescence spectrophotometer (Hitachi Co. Ltd., Ibaraki, Japan). The excitation and emission wavelengths were set to 490 and 520 nm, respectively. After addition of 20 µL cobalt chloride solution (10 mM) to quench the fluorescent intensity of non-capsulated calcein, the fluorescent intensity of encapsulated calcein (F_{in}) was also measured. Finally, in order to disrupt the liposomes completely, the 20 µL of 10 % Triton X-100 was added and the fluorescent intensity after quenching by cobalt

chloride (F_q) was measured. The trapping efficiency of the liposomes was calculated as follows [23].

$$\text{Trapping efficiency (\%)} = [(F_{in} - F_q \times r) / (F_t - F_q \times r)] \times 100$$

Where r is a volume compensation coefficient (r = 1.05).

2.7 Cell culture

Human colon carcinoma Caco-2 cells were obtained from American Type Culture Collection (ATCC, Rockville, CT, USA). Raji cells (B-cell lymphoma line) were a generous gift from Institute of Development, Aging and Cancer, Tohoku University, Sendai, Japan.

Caco-2 cells were grown in DMEM with 100 U/mL penicillin, 100 μg/mL streptomycin, 1 % NEAA, and 10 % heat-incubated FBS at 37 °C in a 5 % CO_2-humidified incubation. Raji cells were cultured in RPMI 1640 medium with 100 U/mL penicillin, 100 μg/mL streptomycin, 1 % NEAA and 10 % heat-incubated FBS.

2.8 Establishment and validation of the small intestinal epithelial cell models

For Caco-2 cell monolayer model, Caco-2 cells (3×10^4 cells/mL) were seeded onto a 12 mm polycarbonate transwell filter insert with 3.0-μm pores and a surface area of 0.6 cm^2 (Millipore Co. Ltd., Billerica, MA, USA). The transwell filter inserts were placed in 24-well cell culture plates. The cells were grown in DMEM (400 μL)

in the apical (AP) chamber and DMEM (600 μL) in the basolateral (BL) chamber. The AP and BL chambers were given fresh DMEM at two-day intervals until use. Caco-2 cells were grown for 20 days (postconfluence) before the experiments.

For M cell monolayer model, the preparation of M cells from Caco-2 cells was performed accoding to the methods of Gullberg *et al.* [17]. Briefly, Raji cells (5×10^5 cells/mL) were suspended in RPMI/DMEM (1:2, v/v) mixture medium and added to the BL chamber of 14-day-old Caco-2 cell monolayer. Coculture of both cells was then maintained for another 6 days.

2.8.1 TEER measurement

To verify the monolayer integrity, the transepithelial electrical resistance (TEER) values were measured using a Millicell® ERS (Millipore Co. Ltd., Billerica, MA, USA). The electrodes were pre-equilibrated in phosphate buffered saline (PBS) at pH 7.4 for 2 h and in DMEM medium for another 30 min before use. The TEER values were measured and recorded every 3 days until day 21. The TEER value was calculated by the following equation.

$$\text{TEER value } (\Omega\cdot\text{cm}^2) = (\text{TEER } (\Omega) - \text{TEER}_{\text{blank}} (\Omega)) \times \text{Area } (\text{cm}^2)$$

Where TEER (Ω) is the value of electrical resistance across Caco-2 or M cell monolayer. $\text{TEER}_{\text{blank}}$ (Ω) is the value of electrical resistance across the transwell filter insert only (without cells). Area is the area of the transwell filter insert, 0.6 cm^2.

2.8.2 Permeability of Lucifer yellow (LY)

LY was dissolved in HBSS containing 10 mM MES and 1 % FBS at pH 6.0. LY solution (0.5 mM, 400 μL) was added to the AP chamber and 600 μL HBSS containing 10 mM HEPES and 1 % FBS at pH 7.4 was applied to the BL chamber of the Caco-2 cell and M-cell monolayers. After incubation at 30, 60, 120 and 180 min in a 5 % CO_2-humidified atomosphere at 37 °C, 50 μL HBSS in BL chamber was collected and the same volume of HBSS was replenished. The collected HBSS was diluted to 1 mL and then the concentration of LY transported into BL chamber was determined by measuring the fluorescent intensity with Hitachi F-2500 fluorescence spectrophotometer. The excitation and emission wavelengths used were 430 and 540 nm, respectively. The apparent permeability coefficient (Papp) was calculated using the following equation [24].

$$P_{app}\ (cm/s) = (\delta Q / \delta t) \times (1 / (A \times C_0)).$$

Where $\delta Q/\delta t$ is the rate of the LY permeation. A is the insert area, 0.6 cm^2, C_0 is the initial concentration of LY, 0.5 mM.

2.8.3 Transport of fluorescent latex beads

The full differentiation of M cell monolayer was confirmed by checking the amount of transported fluorescent latex beads [25]. Before experiment, the fluorescent latex beads were suspended in HBSS (1 % FBS, pH 6.0) and pre-incubated at 4 °C or 37 °C. The AP and BL chambers were washed twice and pre-equilibrated for 30 min

in HBSS (1 % FBS, pH 6.0) in the AP chamber and HBSS (1 % FBS, pH 7.4) in the BL chamber. The fluorescent latex beads in 400 µL HBSS (pH 6.0) was added to the AP chamber while 600 µL HBSS at pH 7.4 was applied in the BL chamber. After incubation at 4 °C or 37 °C for 2 h, the HBSS in the BL chamber was collected and the fluorescent intensity of the transported fluorescent latex beads were determined. The excitation and emission wavelengths were 365 and 415 nm, respectively.

2.8.4 Scanning Electron Microscopy (SEM)

After fully differentiated, the Caco-2 and M cell monolayers were rinsed with PBS for three times, tore with the transwell filter and initially fixed with 2 % paraformaldehyde / 2.5 % glutaraldehyde / 0.05 M cacodylate buffer (pH 7.6) for three hours. Then, rinsed twice in 0.05 % cacodylate buffer (pH 7.6) for 15 minutes, and secondary fixed with 1% osmium-0.05 M cacodylate buffer (pH 7.6) for an hour. Again, rinsed twice in 0.05 % cacodylate buffer (pH 7.6) for 15 minutes, and replaced with 50 % ethanol, 60 % ethanol, 70 % ethanol, 80 % ethanol, 90 % ethanol, 95 % ethanol, 99.5 % ethanol and absolute ethanol in turn for twice every 10 minutes to dryness. Next, the transwell filter was dipped into t-butyl alcohol, frozen and the solvent was vacuum dried. The fixed sample thus obtained was set to disk for SEM. Platinum vanadium was coated with ION SUPATTER JFC-1100 and observed by the SEM (JEOL JSM-5510, Tokyo, Japan).

2.9 Transport and uptake studies of liposomes

The AP and BL chamber in 24-well plate were washed and pre-equilibrated for 30 min at 37 °C in a 5 % CO_2-humidified incubation. One mM calcein encapsulated liposomes in HBSS (400 μL, 1 % FBS, pH 6.0) was added to the AP chamber while the HBSS (600 μL, 1 % FBS, pH 7.4) was applied in the BL chamber. After incubation for 3 h, the HBSS in the BL chamber was collected and by adding 10 % Triton X-100 to disrupt the transported liposomes. Then, cells were washed with PBS, then harvested and lysed. The fluorescent intensity was determined using Hitachi F-2500 fluorescence spectrophotometer. The excitation and emission wavelengths were 490 and 520 nm, respectively.

2.10 Fatty acid composition analysis of phospholipids in differentiated Caco-2 and M cells

The fatty acid composition of PLs in differentiated Caco-2 and M cells were analyzed by GC method. Briefly, at the end of transport and uptake experiments, cells were rinsed twice with ice-cold PBS and then scraped off in PBS followed by centrifugation to collect the cell pellet. Total lipids were extracted following the method of Bligh & Dyer [26]. Individual lipid classes were separated on thin layer chromatography using preparative glass plate coated with silica gel 60 (Darmstadt, Merck, Germany) and developed in petroleum ether-diethyl ether-acetic acid (80:20:1, v/v/v). PLs fraction was visualized by iodine vapor and then the PLs-containing band

was scraped off from the plate. The scraped band was applied to silica gel column and eluted with methanol to remove the silica gel. Methanol eluates were evaporated to obtain PLs. The methyl esters of the fatty acids bound to the PLs were prepared and analyzed by GC following the same method as described in section 2.4 of this study.

2.11 Regulation of tight junctions integrity by liposomes

To investigate the tight junctions integrity in small intestinal epithelial cell monolayers after addition of liposomes consisted of marine complex lipids and soy-PL, TEER measurement was carried out during the treatment with 1 mM liposomes. The TEER values were measured and recorded at 0, 10, 20, 30, 60, 90, 120 and 180 min, respectively.

2.12 Cytotoxicity test of liposomes

After fully differentiated, Caco-2 and M cells were collected from the transwell filter insert and seeded into 96-well plate at 1×10^5 cells/mL in 200 μL growth medium per well. After 24 h, the cells were treated with 1 mM liposomes prepared in this study for 3 h. WST-1 reagent (3.26 mg/ml in 20 mM HEPES including 0.2 mM 1-methoxy PMS) at 20 μL was added in each well. The plates were incubated for another 3 h. The absorbance was subsequently measured at 450 nm versus a 650 nm reference in each well by using SpectraMax M5e microplate reader (Molecular

Devices, Sunnyvale, CA, USA). The cell viability was determined according to the following equation.

Cell viability (%) = ($A_{treated}$ / $A_{control}$) × 100 %

Where $A_{treated}$ and $A_{control}$ are the average absorbance of the treated and control groups, respectively.

2.13 Statistical analysis

All values in this study were expressed as mean ± standard error (SE). All statistical analyses were performed using SPSS software. Data were analyzed using Student's t-test or Tukey's post hoc test. *P* value less than 0.05 was considered statistically significant.

3 Results

3.1 Fatty acid composition of marine and soy phospholipids

Fatty acid composition of PLs extracted from starfish, sea cucumber and soy are shown in **Table 1**. SFP contained 42 % EPA, 8.8 % arachidonic acid (AA) and 6.8 % DHA while SCP included 47.9 % EPA, 11.5 % stearic acid (C18:0) and 6.1 % oleic acid (C18:1). Soy-PL was rich in 62.7 % linoleic acid (C18:2), 18.9 % palmitic acid (C16:0) and 9.7 % oleic acid (C18:1).

3.2 Chemical structure of cerebrosides from starfish and sea cucumber

As shown in **Fig. 1,** the glycosyl group of SFC and SCC was glucose. The main amide-linked fatty acids in SFC were C24:1h (52.2 %), C22:0h (12.4 %) and C24:0h (12.0 %) while the major sphingoid base components were d18:3 (48.6 %) and 4, 8-sphingadienine (d18:2, 39.9 %). SCC contained 68.1 % C24:1h, 20.4 % C23:0h and 11.5 % C22:0h as well as 68.1 % d17:1 and 31.9 % d18:2 (**Table 2**).

3.3 The characterization of liposomes

Five kinds of liposomes were prepared in this study. The average particle sizes of liposomes consisted of SFP/Chol, SCP/Chol, SFP/SFC/Chol, SCP/SCC/Chol and soy-PL/Chol were 168.9 ± 34.4, 174.2 ± 38.6, 189.2 ± 45.5, 184.2 ± 42.8 and 169.1 ± 34.8 nm, respectively (**Table 3**). In addition, as shown in the same table, there were no significant differences in trapping efficiency among the liposomes consisted of SFP/Chol, SCP/Chol or soy-PL/Chol. In addition, the results showed that the liposomes consisted of SFP/SFC/Chol or SCP/SCC/Chol showed higher trapping efficiency than liposomes consisted of SFP/Chol, SCP/Chol and soy-PL/Chol ($P < 0.05$). However, the trapping efficiency of hybrid liposomes remained 7.6 % at the most.

3.4 Integrity of the small intestinal epithelial cell models

Prior to the transport studies with marine complex lipid or soy-PL liposomes, the monolayer integrity of small intestinal epithelial cell models (Caco-2 cell monolayer model and M cell monolayer model) were ensured by four ways, i.e. TEER values, permeability of LY, the amount of transported fluorescent latex beads and the SEM images.

The cell monolayer is considered tight when the TEER value is more than 400 $\Omega \cdot cm^2$ [27]. As shown in **Fig. 2**, with the increasing of incubation time, the TEER values of Caco-2 cell monolayer were elevated significantly. And the average TEER value at day 21 was 594 ± 17.5 $\Omega \cdot cm^2$. However, the TEER values decreased notably after co-cultured with Raji cells for 6 days. This is consistent with the result of previous literature data [28].

LY is commonly employed as a paracellular marker for determining the monolayer integrity of small intestinal epithelial cell models [29]. As shown in **Table 4**, the permeability experiment with LY showed that the Papp value of LY across Caco-2 cell monolayer was 0.9979×10^{-7} cm/s, indicating that the Caco-2 cell monolayer is intact. In addition, this table also illustrated that the Papp value of LY across M cell monolayer was 6.6645×10^{-7} cm/s, which was significantly higher than the Papp value of LY on Caco-2 cell monolayer. But the integrity of the M cell monolayer is not compromised.

Intestinal M cells have been shown to preferentially bind and engulf the hydrophobic polystyrene latex beads [30]. To investigate whether the transport of fluorescent latex beads across Caco-2 and M cell monolayers is temperature-dependent, the amount of transported fluorescent latex beads across Caco-2 and M cell monolayers were measured at 4 °C and 37 °C. As shown in **Fig. 3**, the transport of fluorescent latex beads across M cell monolayer was much higher than Caco-2 cell monolayer at 37 °C. In addition, no significant change was observed in the transport of fluorescent latex beads across Caco-2 cell monolayer at 4 °C in comparison with the result at 37 °C. However, the transport of fluorescent latex beads across M cell monolayer was blocked at 4 °C, which indicates that the fluorescent latex beads were transported by an energy-dependent process.

To further confirm the differentiation of the small intestinal epithelial cell models, the morphological characteristics of Caco-2 and M cell monolayers were observed through SEM. As shown in **Fig. 4A** & **Fig. 4B**, the Caco-2 cells were differentiated into normal small intestinal epithelial cells which were characterized by typical brush border and microvilli. After co-cultured with Raji cells for 6 days, the absence of microvilli was observed in **Fig. 4C** & **Fig. 4D**. Taken together, throughout these evidence, it is suggested that the small intestinal epithelial cell models were established successfully.

3.5 Transport and uptake effects of liposomes in small intestinal epithelial cell models

The transport and uptake of marine complex lipid liposomes across the Caco-2 or M cell monolayer model were measured by the transported calcein amount trapped in the liposomes from AP chamber to BL chamber. As shown in **Fig. 5A**, all the liposomes prepared in this study showed higher transport across the M cell monolayer model than the Caco-2 cell monolayer model ($P < 0.05$). In addition, the transport of liposomes consisted of marine complex lipids across both Caco-2 and M cell monolayer models were superior to soy-PL/Chol liposomes. For Caco-2 cell monolayer model, the transport effects of marine complex lipid liposomes were comparable. However, for M cell monolayer model, hybrid liposomes consisted of SFP/SFC/Chol showed much more potent transport effect than other marine complex lipid liposomes.

On the other hand, our findings in the uptake effects of the marine complex lipid liposomes in small intestinal epithelial cell models revealed that besides the hybrid liposomes consisted of SFP/SFC/Chol, the effects of other marine complex lipid liposomes in both Caco-2 and M cell monolayer models were comparable (**Fig. 5B**). Similarly, the uptake effects of marine complex lipid liposomes were better than soy-PL/Chol liposomes ($P < 0.05$). Moreover, as shown in the same figure, the hybrid liposomes consisted of SFP/SFC/Chol showed much higher uptake than other marine complex lipid liposomes in both Caco-2 and M cell monolayer models.

3.6 Effects of liposomes treatment on the fatty acid profile of phospholipids in small intestinal epithelial cells

Since fatty acids treatment can modulate the fatty acid composition of cell membrane, and PLs are an integral part of cell membrane, the fatty acid composition of PLs in differentiated Caco-2 and M cells after treated with liposomes was analyzed by using GC method. As shown in **Table 5** & **Table 6**, incubation with HBSS did not affect the fatty acid profile of PLs in the differentiated Caco-2 and M cells as compared to the cells which were cultured in DMEM. Marine complex lipid liposomes treatment at the concentration of 1 mM for 3 h tended to increase the EPA content (by 3-fold, $P < 0.05$) in PLs fraction of both differentiated Caco-2 and M cells. The result also revealed that treatment with liposomes led to a slight decrease in the content of palmitic acid in PLs of small intestinal epithelial cells but no obvious differences were observed. In addition, treatment of small intestinal epithelial cells with 1 mM soy-PL liposomes increased the accumulation of linoleic acid significantly while decreasing the content of palmitic acid in PLs of the differentiated Caco-2 and M cells but without statistically significant difference (**Table 5** & **Table 6**).

3.7 Effects of liposomes on tight junctions integrity

Tight junctions are known to regulate the intestinal epithelial permeability by blocking the free diffusion of luminal noxious macromolecules between the apical and basolateral domains of the plasma membrane in intestinal epithelial cells [31]. To investigate whether the liposomes prepared in this study affect the tight junctions integrity of small intestinal epithelial cell monolayer, we measured and calculated the TEER values of Caco-2 and M cell monolayers after co-incubated with liposomes for 0, 10, 20, 30, 60, 90, 120 and 180 min, respectively. The present findings showed that soy-PL liposomes did not decrease the TEER values of Caco-2 and M cell monolayers during the experimental period (**Fig. 6**). Treatment with marine complex lipid liposomes decreased the TEER values of Caco-2 and M cell monolayers in a time-dependent manner. But there were no significant changes on the TEER values of the Caco-2 and M cell monolayers after co-incubated with 1 mM SFP or SCP liposomes for up to 3 h as compared to control. However, the liposomes consisted of SFP/SFC/Chol could decrease the TEER values of Caco-2 and M cell monolayers notably at 120 and 180 min. These data suggest that the hybrid liposomes consisted of SFP/SFC/Chol may open the tight junctions of Caco-2 and M cell monolayers.

3.8 Effects of liposomes on cell viability of small intestinal epithelial cells

To confirm whether the prepared liposomes affect the cell viability of small intestinal epithelial cells, the effects of liposomes on cell viability of differentiated

443 Caco-2 and M cells were measured by using WST-1 assay. As shown in **Fig. 7**, the
444 cell viability of differentiated Caco-2 and M cells were not affected significantly by
445 the liposomes in transport and uptake studies after treated with up to 1mM liposomes
446 for 3 h.
447
448 ## 4 Discussion
449 The aim of this study was to evaluate the transport and uptake effects of marine
450 complex lipid liposomes in small intestinal epithelial cell models. It is well known
451 that the major portion of PLs have been considered to be hydrolyzed in the small
452 intestine by pancreatic phospholipase A_2 with the help of other lipases [1]. Therefore,
453 the transport and uptake effects of liposomes consisted of marine complex lipids or
454 soy-PL in small intestinal epithelial cell models were investigated in the present study.
455 Caco-2 cells and Raji cells were employed to establish the Caco-2 and M cell
456 monolayer models in the present study. To confirm whether the small intestinal
457 epithelial cells are formed, the TEER values, permeability of LY, the amount of
458 transported fluorescent latex beads and the morphological characteristics in Caco-2
459 and M cell monolayer models were investigated. And the results of these experiments
460 suggest that the small intestinal epithelial cell models are well established.
461 It has been proposed that the size of particles plays a key role in the extent of
462 transport across and uptake in the Caco-2 monolayer and the smaller size particles
463 seem to have efficient interfacial interaction with the cell membrane compared to

larger size particles [32]. Desai *et al.* also suggest that the mechanism of uptake of nanoparticles in Caco-2 cells is particle diameter dependent [33]. The average particle sizes of liposomes prepared in this study were from 169 to 189 nm. Evidence demonstrates that nanoparticles of 100-200 nm size acquire the best properties for cellular uptake [32]. In the present study, the transport of liposomes across M cell monolayer model were much higher than Caco-2 cell monolayer model. The results also demonstrated that the liposomes consisted of EPA-PL derived from starfish and sea cucumber showed significantly higher transport and uptake than soy-PL liposomes in both Caco-2 and M cell monolayer models, suggesting the higher absorption of marine complex lipid liposomes in small intestine epithelial cells. It also indicates that the acyl chain composition of PLs should affect the monolayer permeability greatly. In addition, existing evidence suggest that the fatty acids may integrate into cell membrane to change physical properties of cell membrane, and subsequently alter cell membrane fluidity and cell functions in an unsaturation number-dependent manner [34,35]. The present results exhibited that co-incubation with 1 mM marine complex lipid liposomes for 3 h tended to increase the EPA content while treatment with soy-PL liposomes increased the accumulation of linoleic acid in PLs of both differentiated Caco-2 and M cells. Therefore, an increase in unsaturation of PLs fraction in small intestine epithelial cells may be responsible for the higher transport and uptake effects of marine complex lipid liposomes across Caco-2 and M cell monolayer models in comparison with soy-PL liposomes.

Tight junctions between adjacent epithelial cells are considered to create a physiological intercellular barrier which maintains distinct tissue spaces and separate the apical from the lateral plasma membranes [36,37]. Tight junctions are the typical structures in epithelial and endothelial cells and play a key role in controlling the diffusion of some molecules, such as proteins, lipids and toxic compounds, across the intestine. Tight junctions consist of transmembrane and intracellular scaffold proteins. The transmembrane proteins such as occludin creates a permselective barrier in the paracellular pathways by hemophilic and heterophilic interactions with adjacent cells [31,38,39]. The intracellular domains of the transmembrane proteins interact with the intracellular scaffold proteins such as zonula occludens (ZO)-1, which in turn anchor the transmembrane proteins to the actin cytoskeleton [31,40]. These proteins are important to maintain the structure and function of tight junctions. Numerous studies suggest that impairment of the paracellular barrier function has often been related to alterations in the junctional expression and localization of occludin and ZO-1 [41–43]. Usami *et al.* have reported that treatment with 200 μM EPA for 24 h decreases the TEER values and enhances the permeability of Caco-2 cell monolayers [36]. However, another study has shown that 100 μM EPA has no effect on TEER values [44]. Moreover, Jiang *et al.* have suggested that EPA enhances the tight junctions function in endothelial cell monolayer through upregulating the expression of occludin [37]. As for linoleic acid, TEER values as well as occludin staining were unaffected by a chronic treatment with linoleic acid at 50 μM [45]. Our present data revealed that

liposomes consisted of EPA-PL decreased the TEER values of Caco-2 and M cell monolayers for up to 3 h as compared to control but no obvious differences were observed. The results in this study also showed that soy-PL liposomes did not decrease the TEER values of Caco-2 and M cell monolayers during the experimental period. These findings are not consistent with a part of the results from the previous studies performed in Caco-2 cell monolayer model. The differences between the present study and the aforementioned studies may result from differences in the experimental procedure such as different fatty acid concentrations, treatment durations or Caco-2 cell maturation state. Future studies are required to elucidate this discrepancy.

On the other hand, the biological activities of cerebrosides have been reported, but the bioavailability of cerebrosides derived from marine echinoderms in digestive tract are still unknown. Recently, the hybrid liposomes composed of compounds and PLs have received more and more attention. Several studies have reported that the hybrid liposomes could combine the advantages of both compounds and liposomes [46–48]. In addition, it has been reported that drugs encapsulated in liposomes could penetrate across cell membrane effectively [49]. For this reason, the hybrid liposomes consisted of EPA-PL and cerebrosides derived from starfish and sea cucumber were prepared and then their transport and uptake effects in Caco-2 and M cell monolayer models were also evaluated in this study. Our results revealed that the hybrid liposomes consisted of SFP/SFC/Chol showed higher transport across M cell

monolayer as compared to other liposomes. Similarly, the uptake effect of the SFP/SFC/Chol liposomes was much higher than other marine complex lipid liposomes in both Caco-2 and M cell monolayer models. Moreover, treatment with SFP/SFC/Chol liposomes could decrease the TEER values of Caco-2 and M cell monolayers notably. These data suggest that the higher transport and uptake effects of hybrid liposomes consisted of SFP/SFC/Chol may be due to opening the tight junctions of Caco-2 and M cell monolayers. However, further studies are necessary to determine the molecular basis of these findings.

The present data also showed that the cell viability of differentiated Caco-2 and M cells were not affected after treated with up to 1mM marine complex lipid or soy-PL liposomes for 3 h. It indicates that the transport and uptake effects of marine complex lipid or soy-PL liposomes in small intestinal epithelial cells are independent of effects on cell viability.

Conclusion

In summary, Our findings in this study demonstrate that the transport and uptake effects of liposomes consisted of marine complex lipids derived from starfish *A. amurensis* and sea cucumber *C. frondosa* are superior to the soy-PL liposomes in Caco-2 and M cell monolayer models. In addition, the results in this study also reveal that the hybrid liposomes consisted of EPA-PL and cerebrosides isolated from starfish *A. amurensis* exhibit higher transport and uptake effects than other complex lipids in

small intestinal epithelial cells. The prominent transport and uptake effects of marine complex lipid liposomes in Caco-2 and M cell monolayer models may be due to size of particles, an increase in unsaturation of intestinal epithelial cell membrane and affecting the tight junctions of Caco-2 and M cell monolayers.

Acknowledgments

This work was supported by the grants form National Natural Science Foundation of China (NSFC, No.31330060, No.31371757 and No.31201329), NSFC-Shandong Joint Fund for Marine Science Research Centers (U1406402) and the Towa Foundation for Food Science & Research. The author Lei Du also thanks China Scholarship Council (No. 201206330082) for supporting his study in Hokkaido University.

References

1 L. Burri, N. Hoem, S. Banni and K. Berge, *Int. J. Mol. Sci.*, 2012, **13**, 15401–15419.

2 X. Liu, Y. Xue, C. Liu, Q. Lou, J. Wang, T. Yanagita, C. Xue and Y. Wang, *Lipids Health Dis.*, 2013, **12**, 109.

3 K. Fukunaga, Z. Hossain and K. Takahashi, *Nutr. Res.*, 2008, **28**, 635–640.

4 N. Perin, E. Jarocka-Cyrta, M. Keelan, T. Clandinin and A. Thomson, *J. Pediatr. Gastroenterol. Nutr.*, 1999, **28**, 46–53.

5 J. Xu, Y. M. Wang, T. Y. Feng, B. Zhang, T. Sugawara and C. H. Xue, *Biosci. Biotechnol. Biochem.*, 2011, **75**, 1466–1471.

6 H. Oku, S. Wongtangtintharn, H. Iwasaki, M. Inafuku, M. Shimatani and T. Toda, *Cancer Chemother. Pharmacol.*, 2007, **60**, 767–775.

7 H. Oku, C. Li, M. Shimatani, H. Iwasaki, T. Toda, T. Okabe and H. Watanabe, *Cancer Chemother. Pharmacol.*, 2009, **64**, 485–496.

8 E. Zigmond, S. W. Zangen, O. Pappo, M. Sklair-Levy, G. Lalazar, L. Zolotaryova, I. Raz and Y. Ilan, *Am. J. Physiol. Endocrinol. Metab.*, 2009, **296**, E72–78.

9 W. Wang, Y. Wang, H. Tao, X. Peng, P. Liu and W. Zhu, *J. Nat. Prod.*, 2009, **72**, 1695–1698.

10 T. Sugawara, K. Aida, J. Duan and T. Hirata, *J. Oleo Sci.*, 2010, **59**, 387–394.

11 M. E. Díaz de Vivar, A. M. Seldes and M. S. Maier, *Lipids*, 2002, **37**, 597–603.

12 R. B. van Breemen and Y. Li, *Expert Opin. Drug Metab. Toxicol.*, 2005, **1**, 175–185.

13 P. Artursson, K. Palm and K. Luthman, *Adv. Drug Deliv. Rev.*, 2001, **46**, 27–43.

14 A. des Rieux, E. G. E. Ragnarsson, E. Gullberg, V. Préat, Y. J. Schneider and P. Artursson, *Eur. J. Pharm. Sci.*, 2005, **25**, 455–465.

15 J. M. Gamboa and K. W. Leong, *Adv. Drug Deliv. Rev.*, 2013, **65**, 800–810.

16 M. A. Clark, B. H. Hirst and M. A. Jepson, *Adv. Drug Deliv. Rev.*, 2000, **43**, 207–223.

17 E. Gullberg, M. Leonard, J. Karlsson, A. M. Hopkins, D. Brayden, A. W. Baird and P. Artursson, *Biochem. Biophys. Res. Commun.*, 2000, **279**, 808–813.

18 X. Liu, J. Cui, Z. Li, J. Xu, J. Wang, C. Xue and Y. Wang, *Eur. J. Lipid Sci. Technol.*, 2014, **116**, 255–265.

19 J. Folch, M. Lees and G.H. Sloane Stanley, *J. Biol. Chem.*, 1957, **226**, 497–509.

20 J. Xu, S. Guo, L. Du, Y. M. Wang, T. Sugawara, T. Hirata and C.H. Xue, *J. Oleo Sci.*, 2013, **62**, 133–142.

21 A. F. Prevot and F.X. Mordoret. *Rev. Fse. Corps. Gras.*, 1976, **23**, 409–423.

22 A. D. Bangham, M. M. Standish and J. C. Watkins, *J. Mol. Biol.*, 1965, **13**, 238–252.

23 N. Oku, D. A. Kendall and R. C. MacDonald, *Biochim. Biophys. Acta-Biomembr.*, 1982, **691**, 332–340.

24 S. Hemmersbach, S. S. Brauer, S. Hüwel, H. J. Galla and H. U. Humpf, *J. Agric. Food Chem.*, 2013, **61**, 7932–7940.

25 K. Murakawa, K. Fukunaga, M. Tanouchi, M. Hosokawa, Z. Hossain and K. Takahashi, *J. Oleo Sci.*, 2007, **56**, 179–188.

26 E. G. Bligh and W. J. Dyer, *Can. J. Biochem. Physiol.*, 1959, **37**, 911–917.

27 A. Matthias, J. T. Blanchfield, K. G. Penman, I. Toth, C. S. Lang, J. J. Voss and R. P. Lehmann, *J. Clin. Pharm. Ther.*, 2004, **29**, 7–13.

28 A. des Rieux, V. Fievez, I. Théate, J. Mast, V. Préat and Y. J. Schneider, *Eur. J. Pharm. Sci.*, 2007, **30**, 380–391.

29 L. Zhang, Y. Zheng, M. S. S. Chow and Z. Zuo, *Int. J. Pharm.*, 2004, **287**, 1–12.

30 H. Liu, C. K. Meagher, C. P. Moore and T. E. Phillips, *Invest. Ophthalmol. Vis. Sci.*, 2005, **46**, 4217–4223.

31 T. Suzuki, *Cell. Mol. Life Sci.*, 2013, **70**, 631–659.

32 K. Y. Win and S. S. Feng, *Biomaterials*, 2005, **26**, 2713–2722.

33 M. P. Desai, V. Labhasetwar, E. Walter, R. J. Levy and G. L. Amidon, *Pharm. Res.*, **14**, 1568–1573.

34 X. Yang, W. Sheng, G. Y. Sun and J. C. M. Lee, *Neurochem. Int.*, 2011, **58**, 321–329.

35 M. Ibarguren, D. J. López and P. V Escribá, *Biochim. Biophys. Acta*, 2014, **1838**, 1518–1528.

36 M. Usami, K. Muraki, M. Iwamoto, A. Ohata, E. Matsushita and A. Miki, *Clin. Nutr.*, 2001, **20**, 351–359.

37 W. G. Jiang, R. P. Bryce, D. F. Horrobin and R. E. Mansel, *Biochem. Biophys. Res. Commun.*, 1998, **244**, 414–420.

38 M. Furuse, T. Hirase, M. Itoh, A. Nagafuchi, S. Yonemura and S. Tsukita, *J. Cell Biol.*, 1993, **123**, 1777–1788.

39 L. González-Mariscal, A. Betanzos, P. Nava and B.E. Jaramillo, *Prog. Biophys. Mol. Biol.*, 2003, **81**, 1–44.

40 M. Furuse, M. Itoh, T. Hirase, A. Nagafuchi, S. Yonemura and S. Tsukita, *J. Cell Biol.*, 1994, **127**, 1617–1626.

41 I. C. McCall, A. Betanzos, D. A. Weber, P. Nava, G. W. Miller and C. A. Parkos, *Toxicol. Appl. Pharmacol.*, 2009, **241**, 61–70.

42 C. B. Collares-Buzato, M. A. Jepson, N. L. Simmons and B. H. Hirst, *Eur. J. Cell Biol.*, 1998, **76**, 85–92.

43 S. Tsukita, M. Furuse and M. Itoh, *Nat. Rev. Mol. Cell Biol.*, 2001, **2**, 285–293.

44 O. Rosella, A. Sinclair and P. R. Gibson, *J. Gastroenterol. Hepatol.*, 2000, **15**, 626–631.

45 H. M. Roche, A. M. Terres, I. B. Black, M. J. Gibney and D. Kelleher, *Gut*, 2001, **48**, 797–802.

644 46 H. Kitajima, Y. Komizu and R. Ueoka, *Bioorg. Med. Chem. Lett.*, 2012, **22**,
645 1784–1787.

646 47 Y. Komizu, H. Ueoka, K. Goto and R. Ueoka, *Int. J. Nanomedicine*, 2011, **6**,
647 1913–1920.

648 48 M. S. El-Samaligy, N. N. Afifi and E. A. Mahmoud, *Int. J. Pharm.*, 2006, **319**,
649 121–129.

650 49 K. Iwanaga, S. Ono, K. Narioka, M. Kakemi, K. Morimoto, S. Yamashita, Y.
651 Namba and N. Oku, *J. Pharm. Sci.*, 1999, **88**, 248–252.

652

Figure captions and Table

Fig. 1 The chemical structures of starfish cerebrosides (SFC) and sea cucumber cerebrosides (SCC).

Fig. 2 Changes in TEER values in Caco-2 and M cell monolayers. TEER values in Caco-2 and M cell monolayers were measured using a Millicell® ERS. Value are expressed as mean ± SE (n=4).

Fig. 3 Phagocytosis of fluorescent latex beads on Caco-2 and M cell monolayers at 4 °C or 37 °C. Values are expressed as mean ± SE (n=4), different letters indicate significant difference at $P < 0.05$ among each value determined by Tukey's post hoc test.

Fig. 4 Scanning electronic micrographs of Caco-2 (A&B) and M cell monolayers (C&D).

Fig. 5 Effects of individual liposomes on transport (A) and uptake (B) in Caco-2 and M cell monolayer models. One mM calcein encapsulated liposomes were added to the AP chamber of Caco-2 and M cell monolayers. The transported liposomes in the BL chamber and the absorbed liposomes into differentiated Caco-2 or M cells were determined using fluorescence spectrophotometer after 3 h incubation at 37 °C. The fluorescent intensity was measured at excitation and emission wavelengths of 490 and 520 nm, respectively. Values are expressed as mean ± SE (n=4), different letters indicate significant difference at $P < 0.05$ among each value determined by Tukey's post hoc test.

Fig. 6 Changes in TEER values in Caco-2 cell (A) and M cell monolayer (B) after

treated with individual liposomes. One mM liposomes were added to the AP chamber of Caco-2 cell or M cell monolayer for up to 180 min. TEER value were measured at 0, 10, 20, 30, 60, 90, 120 and 180 min, respectively. The relative TEER values were calculated as a ratio of the TEER values of HBSS treatment at each time point. Values are expressed as mean ± SE (n=4), $^{*}P < 0.05$ versus HBSS treatment.

Fig. 7 Effects of individual liposomes on the cell viability of differentiated Caco-2 (A) and M cells (B). The differentiated Caco-2 and M cells were collected from the transwell filter insert and seeded into 96-well plate at 1×10^5 cells/mL in 200 μL growth medium per well. After incubation for 24 h, the cells were treated with 1 mM liposomes for 3 h. Control cells were treated with HBSS. Values are expressed as mean ± SE (n=4).

Table 1 Fatty acid composition of the marine and soy phospholipids. Values are expressed as mean ± SE (n=3).

Table 2 Fatty acid and sphingoid base composition of cerebrosides obtained from starfish and sea cucumber which were analyzed by GC-MS. Values are expressed as mean ± SE (n=3), different letters indicate significant difference at $P < 0.05$ among each value determined by Tukey's post hoc test.

Table 3 Characterization of the individual liposomes prepared in this study.

Table 4 Transport of 0.5 mM LY across small intestinal epithelial cell models.

Table 5 Fatty acid composition of the phospholipid fractions in differentiated Caco-2 cells after treated with the individual liposomes. Values are expressed as mean ± SE (n=4), different letters in the same row indicate significant difference at $P < 0.05$

among each value determined by Tukey's post hoc test.

Table 6 Fatty acid composition of the phospholipid fractions in M cells after treated with the individual liposomes. Values are expressed as mean ± SE (n=4), different letters in the same row indicate significant difference at $P < 0.05$ among each value determined by Tukey's post hoc test.

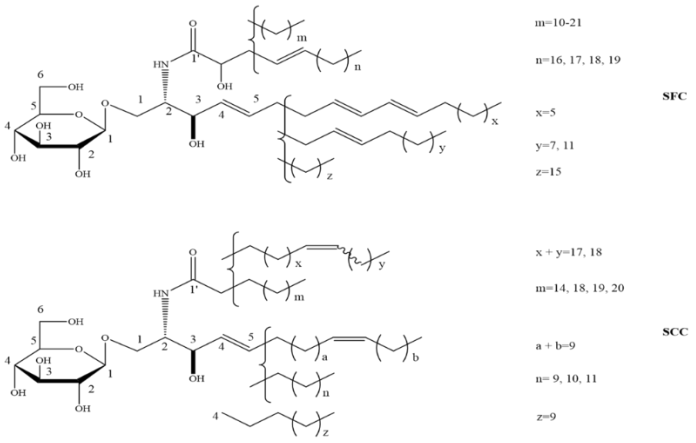

Fig. 1 The chemical structures of starfish cerebrosides (SFC) and sea cucumber cerebrosides (SCC).

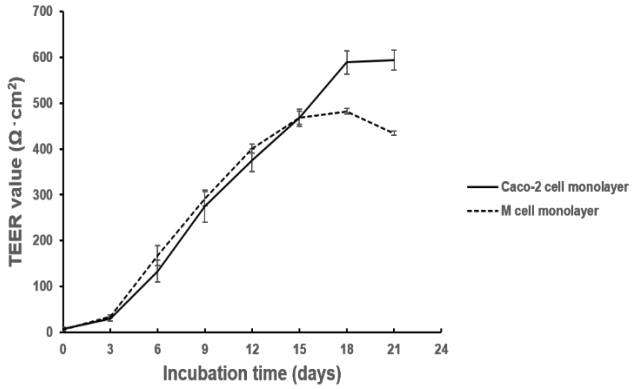

Fig. 2 Changes in TEER values in Caco-2 and M cell monolayers.

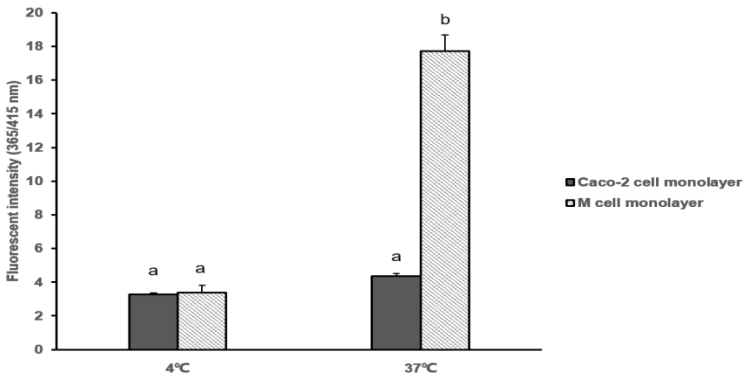

Fig. 3 Phagocytosis of fluorescent latex beads on Caco-2 and M cell monolayers at 4 ˚C or 37 ˚C.

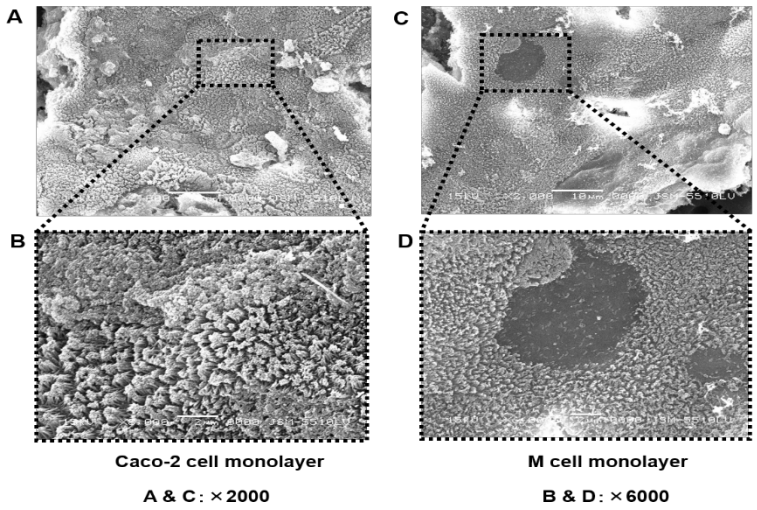

Fig. 4 Scanning electronic micrographs of Caco-2 (A&B) and M cell monolayers (C&D).

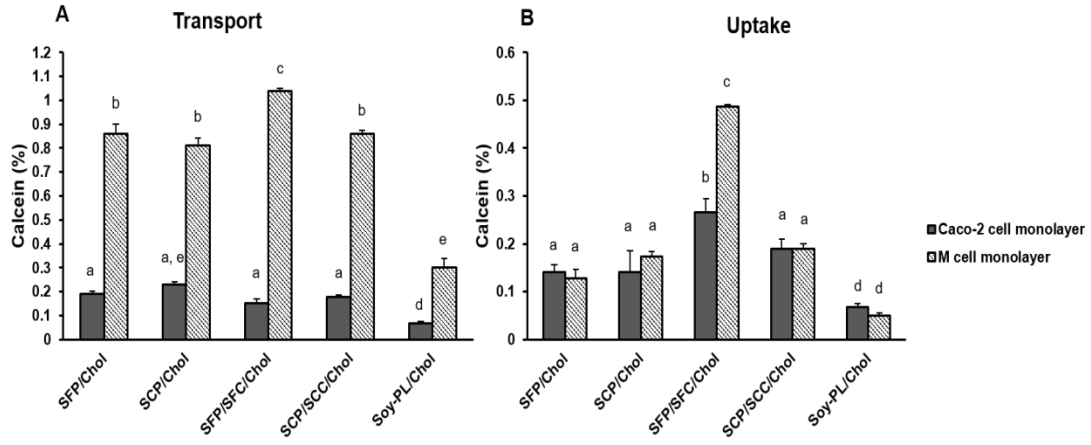

Fig. 5 Effects of individual liposomes on transport (A) and uptake (B) in Caco-2 and M cell monolayer models.

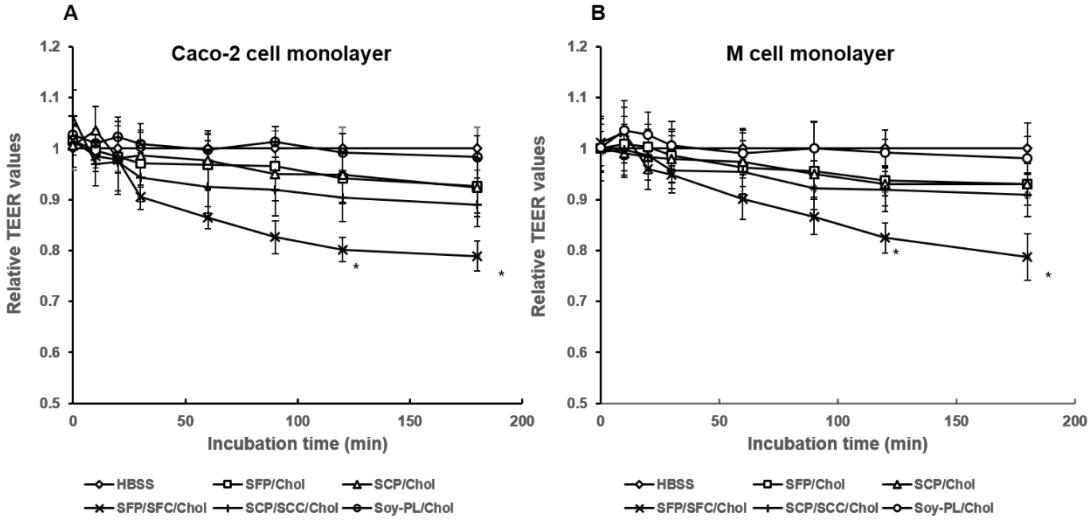

Fig. 6 Changes in TEER values in Caco-2 cell (A) and M cell monolayer (B) after treated with individual liposomes.

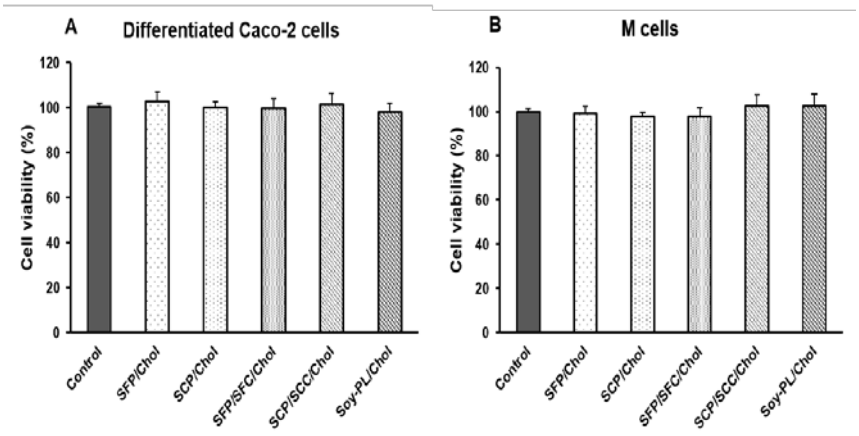

Fig. 7 Effects of individual liposomes on the cell viability of differentiated Caco-2 (A) and M cells (B).

Table 1 Fatty acid composition of the marine and soy phospholipids.

Fatty acid (%)	SFP	SCP	Soy-PL
C14:0	0.7 ± 0.0	0.3 ± 0.0	0.1 ± 0.0
C16:0	3.4 ± 0.2	5.5 ± 0.2	18.9 ± 0.3
C16:1	3.2 ± 0.2	4.2 ± 0.0	0.2 ± 0.0
C18:0	8.5 ± 0.3	11.5 ± 0.5	2.4 ± 0.2
C18:1	6.5 ± 0.3	6.1 ± 0.3	9.7 ± 0.6
C18:2	-	0.4 ± 0.0	62.7 ± 1.1
C18:3 n-3	-	0.6 ± 0.0	3.6 ± 0.4
C20:1	5.6 ± 0.2	7.8 ± 0.2	0.1 ± 0.0
C20:2	0.5 ± 0.0	-	-
C20:3	0.1 ± 0.0	-	-
C20:4 n-6 (AA)	8.8 ± 0.1	4.7 ± 0.1	-
C20:5 n-3 (EPA)	42.0 ± 0.8	47.9 ± 0.8	-
C22:6 n-3 (DHA)	6.8 ± 0.4	2.1 ± 0.4	-
Others	13.9 ± 0.5	8.9 ± 0.3	2.3 ± 0.4

Table 2 Fatty acid and sphingoid base composition of cerebrosides obtained from starfish and sea cucumber which were analyzed by GC-MS.

	Fatty acid	Ratio of peak areas (%)	Sphingoid base	Ratio of peak areas (%)
SFC	C16:0h	9.5		
	C18:0h	6.7	d18:2	39.9
	C22:0h	12.4	d18:3	48.6
	C24:0h	12.0	d22:1	5.9
	C24:1h	52.2	d22:2	5.6
	C25:1h	7.2		
SCC	C22:0h	11.5	d17:1	68.1
	C23:0h	20.4	d18:2	31.9
	C24:1h	68.1		

Table 3 Characterization of the individual liposomes prepared in this study

Lipid composition (mol/mol/mol)	Average particle size (nm)	Trapping efficiency (%)
SFP/Chol = 1:1	168.9 ± 34.4	5.3 ± 0.3[a]
SCP/Chol = 1:1	174.2 ± 38.6	5.7 ± 0.2[a]
SFP/SFC/Chol = 1:1:2	189.2 ± 45.5	7.2 ± 0.3[b]
SCP/SCC/Chol = 1:1:2	184.2 ± 42.8	7.6 ± 0.2[b]
Soy-PL/Chol = 1:1	169.1 ± 34.8	5.4 ± 0.3[a]

Table 4 Transport of 0.5 mM LY across small intestinal epithelial cell models

	Papp ($\times 10^{-7}$(cm/s))
Caco-2 cell monolayer	0.9979
M cell monolayer	6.6645

Table 5 Fatty acid composition of the phospholipid fractions in differentiated Caco-2 cells after treated with the individual liposomes.

Fatty acid (%)	DMEM	HBSS	SFP/Chol	SCP/Chol	SFP/SFC/ Chol	SCP/SCC/ Chol	Soy-PL/ Chol
C14:0	1.8 ± 0.2	1.8 ± 0.1	1.6 ± 0.1	1.7 ± 0.1	1.6 ± 0.1	1.7 ± 0.1	1.8 ± 0.2
C16:0	26.4 ± 0.8	26.8 ± 0.7	26.3 ± 0.7	25.6 ± 0.7	26.2 ± 0.7	25.5 ± 0.8	25.6 ± 0.8
C16:1	12.5 ± 0.4	12.5 ± 0.3	12.8 ± 0.3	12.7 ± 0.3	12.8 ± 0.3	12.9 ± 0.4	12.2 ± 0.3
C18:0	10.6 ± 0.3	10.2 ± 0.3	10.4 ± 0.3	10.5 ± 0.4	10.2 ± 0.3	10.5 ± 0.3	10.4 ± 0.3
C18:1	28.8 ± 0.6	29.0 ± 0.8	28.6 ± 0.7	28.4 ± 0.8	28.7 ± 0.6	28.5 ± 1.0	29.2 ± 0.8
C18:2	0.9 ± 0.1[a]	0.6 ± 0.1[a]	0.8 ± 0.1[a]	1.0 ± 0.1[a]	0.8 ± 0.1[a]	0.9 ± 0.1[a]	2.4 ± 0.2[b]
C18:3 n-3	1.2 ± 0.2	1.2 ± 0.1	1.2 ± 0.1	1.4 ± 0.2	1.3 ± 0.1	1.4 ± 0.2	1.2 ± 0.1
C20:0	1.6 ± 0.2	1.8 ± 0.3	1.9 ± 0.3	1.4 ± 0.2	1.4 ± 0.2	1.3 ± 0.2	1.6 ± 0.2
C20:1	2.3 ± 0.2	2.1 ± 0.2	2.4 ± 0.2	2.1 ± 0.2	2.3 ± 0.2	2.2 ± 0.2	2.0 ± 0.2
C20:4n-6 (AA)	2.6 ± 0.2	2.5 ± 0.2	3.0 ± 0.2	3.2 ± 0.2	2.9 ± 0.1	3.1 ± 0.1	2.2 ± 0.1
C20:5 n-3 (EPA)	0.8 ± 0.1[a]	0.9 ± 0.1[a]	2.2 ± 0.1[b]	2.4 ± 0.1[b]	2.5 ± 0.2[b]	2.4 ± 0.1[b]	0.8 ± 0.1[a]
C22:6 n-3 (DHA)	1.2 ± 0.1	1.1 ± 0.1	1.5 ± 0.2	1.2 ± 0.1	1.6 ± 0.2	1.3 ± 0.1	1.1 ± 0.1
Others	8.3 ± 0.6	9.5 ± 0.5	7.3 ± 0.5	8.4 ± 0.5	7.7 ± 0.4	7.3 ± 0.4	9.5 ± 0.4

Table 6 Fatty acid composition of the phospholipid fractions in M cells after treated with the individual liposomes.

Fatty acid (%)	DMEM	HBSS	SFP/Chol	SCP/Chol	SFP/SFC/ Chol	SCP/SCC/ Chol	Soy-PL/ Chol
C14:0	2.0 ± 0.1	2.0 ± 0.1	1.8 ± 0.1	2.0 ± 0.2	1.9 ± 0.1	1.8 ± 0.1	1.9 ± 0.1
C16:0	27.2 ± 0.4	27.1 ± 0.4	26.4 ± 0.4	26.1 ± 0.4	26.2 ± 0.4	26.1 ± 0.4	25.5 ± 0.3
C16:1	11.6 ± 0.2	11.6 ± 0.2	11.8 ± 0.2	11.6 ± 0.2	11.7 ± 0.2	11.6 ± 0.2	11.5 ± 0.2
C18:0	10.9 ± 0.3	11.1 ± 0.3	10.2 ± 0.3	10.4 ± 0.3	10.2 ± 0.2	10.4 ± 0.3	10.1 ± 0.2
C18:1	29.9 ± 0.4	29.9 ± 0.4	30.1 ± 0.5	30.1 ± 0.4	30.1 ± 0.4	30.2 ± 0.5	30.2 ± 0.4
C18:2	1.0 ± 0.1[a]	1.1 ± 0.1[a]	0.9 ± 0.1[a]	1.0 ± 0.1[a]	1.0 ± 0.1[a]	1.2 ± 0.1[a]	2.2 ± 0.2[b]
C18:3 n-3	1.1 ± 0.1	1.1 ± 0.1	1.2 ± 0.1	1.1 ± 0.1	1.3 ± 0.2	1.3 ± 0.1	1.1 ± 0.1
C20:0	1.8 ± 0.1	1.9 ± 0.2	1.6 ± 0.1	1.8 ± 0.2	1.4 ± 0.1	1.5 ± 0.1	1.9 ± 0.2
C20:1	2.0 ± 0.1	2.0 ± 0.1	2.0 ± 0.1	1.9 ± 0.1	2.0 ± 0.2	1.9 ± 0.1	1.9 ± 0.1
C20:4n-6 (AA)	2.8 ± 0.1	2.9 ± 0.1	3.3 ± 0.2	3.2 ± 0.2	3.3 ± 0.2	3.1 ± 0.2	2.9 ± 0.2
C20:5 n-3 (EPA)	0.8 ± 0.1[a]	0.8 ± 0.1[a]	2.1 ± 0.1[b]	2.3 ± 0.1[b]	2.4 ± 0.2[b]	2.3 ± 0.1[b]	0.9 ± 0.1[a]
C22:6 n-3 (DHA)	1.1 ± 0.1	1.1 ± 0.1	1.4 ± 0.1	1.2 ± 0.1	1.4 ± 0.1	1.2 ± 0.1	1.0 ± 0.1
Others	7.8 ± 0.5	7.4 ± 0.5	7.2 ± 0.4	7.3 ± 0.5	7.1 ± 0.5	7.4 ± 0.5	8.8 ± 0.5